

Performance analysis of a solid oxide fuel cell with reforming and water-shift reaction

Ping Yuan, Syu-Fang Liu, and Ming-Jun Kuo

Abstract— This study investigates the effect of reforming reaction and water-shift reactions on the performance of a SOFC stack. This study utilizes a software package to solve the cell temperature and current density distribution of each stack in this 10-stack SOFC. The results show that the reforming reaction and water-shift reaction can effectively promote the total power and drop the current density deviation, but slightly affect the average cell temperature and cell temperature deviation. Therefore, these two reactions are advanced for the operation of a SOFC stack.

Keywords— *Reforming reaction, Water-shift reaction, Cell temperature, Current density, Solid oxide fuel cell*

I. Introduction

A solid oxide fuel cell (SOFC) includes anodes, cathodes, solid electrolytes, and interconnectors. Its operating temperature is between 600 and 1000°C, and the fuel can be many types such as methane or ethanol. Because the electrolyte is solid, the structure of SOFC stack can easily be formed as different shapes, which generally are cylindrical and plate shape. The plate type of SOFC stack is wider application due to its ease for stacking.

For producing higher power, the reaction area of a SOFC is large due to the benefit of its solid electrolyte, and hence the temperature difference on the reaction area becomes obvious and important for the performance and life of the fuel cell. In the performance analysis of a SOFC, most literature utilize numerical methods, and can be classified three kinds: the three-dimensional analysis for one fuel channel, one air channel, as well as the anode, cathode, and electrolyte between the two channels [1-3]; two-dimensional analysis for the whole reaction area [4-5]; three-dimensional analysis for the whole stacks of a SOFC [6-8]. Because the three-dimensional analysis for a SOFC stack needs large of calculating memories and time, the research results are published after another till recent.

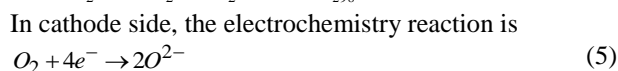
As mentioned before, the SOFC has high operating temperature and can use the methane as the fuel, so the hydrogen concentration will be affected by the other reactions in the anode side except the main electrochemistry reaction, such as the reforming reaction and water-shift reaction. In the research of reforming reaction in a SOFC, most literature builds the theoretical model of reforming reaction, and

discusses the effect of reforming reaction on the performance of the SOFC [9-11]. In the research of water-shift reaction, there are literature utilizes experimental method to find the reaction rate expression and its parameters [12-14]. This study plans to cite the reforming reaction model from literature [11], and water-shift reaction model from literature [13].

In the previous literature focusing on the analysis of a SOFC stack [6-8], most of them do not consider the reforming reaction and water-shift reaction. Therefore, this study investigates the effect of reforming reaction and water-shift reaction on the thermal and electrical performance of a SOFC stack. The results of this study will provide a valuable reference for an engineer in the design of a solid oxide fuel cell.

II. Analysis

This study considers the species of fuel including the CH₄, H₂O, CO, H₂, CO₂, and N₂, as well as air including O₂ and N₂. In anode side, the reactions include the main electrochemistry, reforming, and water-shift reactions.



This study neglects the variation of all variables along the thickness direction in each stack, because the thickness is much less than the size of reaction surface side. Therefore, the analysis of each stack is two-dimensional problem. This study analyzes every stack repeatedly and gets the temperature field and current density field. Figure 1 shows the schematic diagram of a SOFC with multi-stacks. Meanwhile, the superscript *k* stands for the stack number.

This study builds the governing equation of mass, energy, and electrochemistry for each stack, because the feature of repeating layer in a SOFC stack. The following are the mass conservation equations of each stack.

In anode,

$$\left(\frac{1}{L_y} \frac{d(n_j X_j)}{dx} \right)^k = (S_j)^k \quad (6)$$

In cathode,

Ping Yuan*, Syu-Fang Liu, and Ming-Jun Kuo
Lee Ming Institute of Technology
Taipei, Taiwan

$$\left(\frac{1}{L_x} \frac{d(n_a X_j)}{dy}\right)^k = (S_j)^k \quad (7)$$

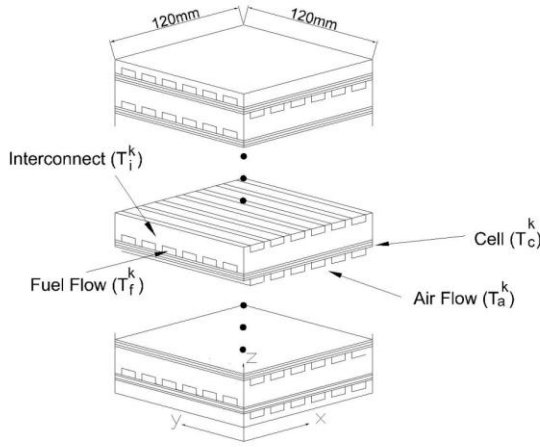


Fig. 1 Schematic diagram of a SOFC with multi-stacks

Meanwhile, the S_j represents the reaction rate of reactants and products, and the superscript k is stack number. The reaction rate of each species in anode are as following.

$$S_{H_2} = -\frac{i}{2F} + 3R_{reform} + R_{shift}, \quad S_{H_2O} = \frac{i}{2F} - R_{reform} - R_{shift}$$

$$S_{CH_4} = -R_{reform}, \quad S_{CO} = -\frac{i}{2F} + R_{reform} - R_{shift}, \quad S_{CO_2} = \frac{i}{2F} + R_{shift} \quad (8)$$

The reaction rate of each species in cathode is as following.

$$S_{O_2} = -\frac{i}{4F} \quad (9)$$

The calculation of reforming reaction rate is cited from literature [11].

$$-R_{CH_4} = k_f e^{\left(\frac{E_{af}}{RT}\right)} \left[P_{CH_4} P_{H_2O} - \frac{P_{CO} P_{H_2}^3}{K_{eq, reform}} \right] \quad (\text{mol s}^{-1}) \quad (10)$$

$$K_{eq, reform} = e^{\left(\frac{\Delta G^0}{RT}\right)} \quad (11)$$

Meanwhile, $E_{af}=94950 \text{ J mol}^{-1}$ and $k_f=9110 \text{ mol s}^{-1} \text{ atm}^2$. The calculation of water-shift reaction rate is cited from literature [13].

$$R_{CO} = 2.96 \times 10^5 e^{\left(\frac{-47400}{RT}\right)} \left[P_{CO} P_{H_2O} - \frac{P_{CO_2} P_{H_2}}{K_{eq, shift}} \right] \quad (12)$$

$$K_{eq, shift} = e^{\left(\frac{-45778}{T} - 4.33\right)} \quad (13)$$

The energy conservation equations of a SOFC stack are as following

For the fuel

$$\frac{d}{dx} (\sum n_j X_j c_{p,j} T_j)^k = (ha)_{-f} (T_i^k - T_c^k) + (ha)_{-f} (T_c^k - T_f^k) + \frac{i}{4F} c_{p,O_2} T_c^k + \dot{q}_{reform}^k + \dot{q}_{shift}^k \quad (14)$$

For the air

$$\frac{d}{dy} (\sum n_a X_j c_{p,j} T_a)^k = (ha)_{-a} (T_i^{k+1} - T_c^k) + (ha)_{-a} (T_c^k - T_a^k) - \frac{i}{4F} c_{p,O_2} T_c^k \quad (15)$$

For the cell including anode, cathode, and electrolyte

$$-(k\delta)_c \frac{\partial^2 T_c^k}{\partial x^2} - (k\delta)_c \frac{\partial^2 T_c^k}{\partial y^2} = (ka)_{-c} \frac{(T_i^k - T_c^k)}{\delta_{-c}} + (ka)_{-c} \frac{(T_c^{k+1} - T_c^k)}{\delta_{-c}} + (ha)_{-f} (T_f^k - T_c^k) \quad (16)$$

$$+ (ha)_{-a} (T_a^k - T_c^k) + \frac{i}{4F} c_{p,O_2} T_c^k - \frac{i}{4F} c_{p,O_2} T_c^k + \dot{q}_{reac}^k$$

For the inter-connector

$$-(k\delta)_i \frac{\partial^2 T_i^k}{\partial x^2} - (k\delta)_i \frac{\partial^2 T_i^k}{\partial y^2} = (ka)_{-c} \frac{(T_c^k - T_i^k)}{\delta_{-c}} + (ka)_{-c} \frac{(T_c^{k+1} - T_i^k)}{\delta_{-c}} + (ha)_{-f} (T_f^k - T_i^k) \quad (17)$$

$$+ (ha)_{-a} (T_a^{k+1} - T_i^k)$$

Meanwhile, the subscript f is fuel, subscript a is air, subscript i is inter-connector, subscript c is the cell. This study considers the boundary of the stack is adiabatic, and the top and bottom facing the surrounding is constant temperature.

$$\frac{\partial^2 T_c^k}{\partial x^2} = \frac{\partial^2 T_c^k}{\partial y^2} = 0, \quad \frac{\partial^2 T_i^k}{\partial x^2} = \frac{\partial^2 T_i^k}{\partial y^2} = 0, \quad (18)$$

$$T_i^k = T_0, \quad k=\text{bottom and top inter-connector} \quad (19)$$

where the T_0 is a constant temperature of 625°C .

The electrochemical equations of each stack of SOFC are as follows

$$E^k - V^k = V_{ohm}^k + V_{act}^k + V_{con}^k \quad (20)$$

$$E^k = E_0^k + \frac{RT_c^k}{2F} \ln \left(\frac{P_{H_2}^k P_{O_2}^{0.5}}{P_{H_2O}^k} \right) \quad (21)$$

$$E_0^k = 1.2723 - 2.7654 \times 10^{-4} T_c^k \quad (22)$$

Meanwhile, the E^k is Nernst voltage of k -th stack, the E_0^k is the reversible voltage under standard condition, the V^k is operation voltage, the V_{ohm}^k is Ohm polarization, the V_{act}^k is activating polarization, V_{con}^k is the concentration polarization. The polarizations are expressed in the following.

$$V_{ohm}^k = i^k r^k \quad (23)$$

$$V_{act}^k = \frac{RT_c^k}{2F} \sinh^{-1} \left(\frac{i^k}{2i_{0,anode}^k} \right) + \frac{RT_c^k}{2F} \sinh^{-1} \left(\frac{i^k}{2i_{0,cathode}^k} \right) \quad (24)$$

$$V_{con}^k = -\frac{RT_c^k}{2F} \ln \left[\frac{1 - (RT_c^k / 2F) (\delta_{anode}^k / D_{anode}^k) (\delta_{H_2}^k) \cdot i^k}{1 + (RT_c^k / 2F) (\delta_{anode}^k / D_{anode}^k) (\delta_{H_2O}^k) \cdot i^k} \right] \quad (25)$$

In the above governing equations, there are six unknown variables: concentration of species, fuel temperature, air temperature, cell temperature, inter-connector temperature, and current density. These variables are functions of x , y , and k , as well as have interaction between stacks through the heat transfer. When the operation voltage is set, this study can solve the equations of (6)-(25). Once the SOFC stack is series connection, this study can easily convert the distribution of current density to distribution of operation voltage according to the unchanged power per area.

Authors have confirmed the accuracy of the software of FlexPDE in the application of a SOFC unit [15-17]. Therefore, this study utilizes the software to solve the governing equations of each stack repeatedly and get the solutions when the relative error of variables satisfies the criteria. For accuracy comparison, this study applies the same condition of

literature [16] to solve a SOFC stack without reforming and water-shift reaction, and compares the results with that in literature. This comparison support the software is reliable.

III. Results and Discussion

This study considers the SOFC has 10 stacks, and investigates the effect of reforming reaction and water-shift reaction on the performance of a SOFC stack. Other parameters are same to the previous literature [16] except the species of fuel and the size of reaction area. Figure 2 depicts the current density distribution with or without reforming and water-shift reactions when the fuel inlet mole flow rate is 0.09 mol/s. The current density near the inlet of fuel in Fig. 2(c) and 2(d) is higher than that in Fig. 2(a) and 2(b). This phenomenon is induced by the water-shift reaction, because this reaction is a rapid reaction and produces hydrogen in the inlet of the fuel. Moreover, the reforming reaction produces more hydrogen, so the lowest current density in Fig. 2(b) and 2(c) is higher than that in Fig. 2(a) and 2(d), respectively. Because both reforming and water-shift reactions produce hydrogen, the current density of all SOFC stack in Fig. 2(c) is higher than that in Fig. 2(b).

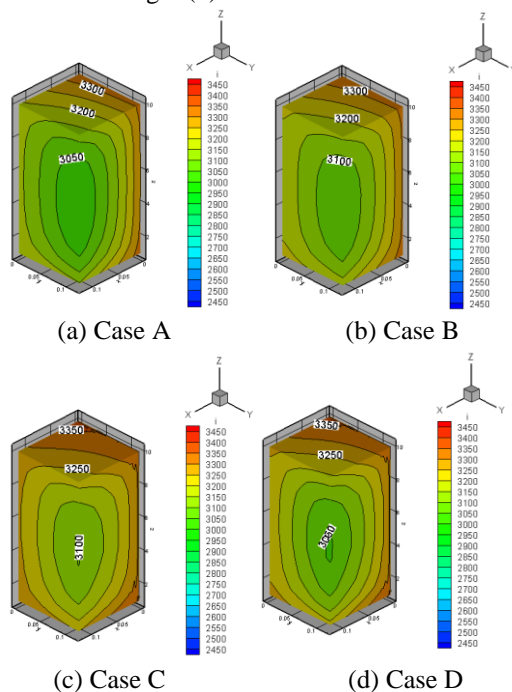


Fig. 2 Current density distribution with or without reforming and water-shift reactions when the fuel inlet mole flow rate is 0.09 mol/s, (a) without reforming and water-shift reaction, (b) with reforming and without water-shift reaction, (c) with reforming and water-shift reaction, (d) without reforming and with water-shift reaction.

Figure 3 shows the cell temperature distribution with or without reforming and water-shift reactions when the fuel inlet mole flow rate is 0.09 mol/s. Because there is no water-shift reaction in Fig. 3(a) and 3(b), their cell temperature near the

fuel inlet is similar to each other. In the exit region in Fig. 3(a) and 3(b), the cell temperature in Fig. 3(b) is lower than that in Fig. 3(a), because it exists the reforming reaction in Fig. 3(b), which is an endothermic reaction. Both Fig. 3(c) and 3(d) contain the water-shift reaction, so their cell temperature near the fuel inlet region are similar. Because the water-shift reaction is an exothermic reaction, the cell temperature near the fuel inlet region in Fig. 3(c) and 3(d) is higher than that in Fig. 3(a) and 3(b). Moreover, the cell temperature in the exit region in Fig. 3(b) and 3(c) is lower than that in Fig. 3(a) and 3(d) because of the endothermic reforming reaction. Due to combined effect of the exothermic water-shift and endothermic reforming reaction, the hot spot of cell temperature in Fig. 3(d) is the highest and that in Fig. 3(b) is the lowest. Moreover, the cell temperature in Fig. 3(c) is lower than that in Fig. 3(a), because the quantity of endothermic of reforming reaction is larger than that of exothermic of water-shift reaction.

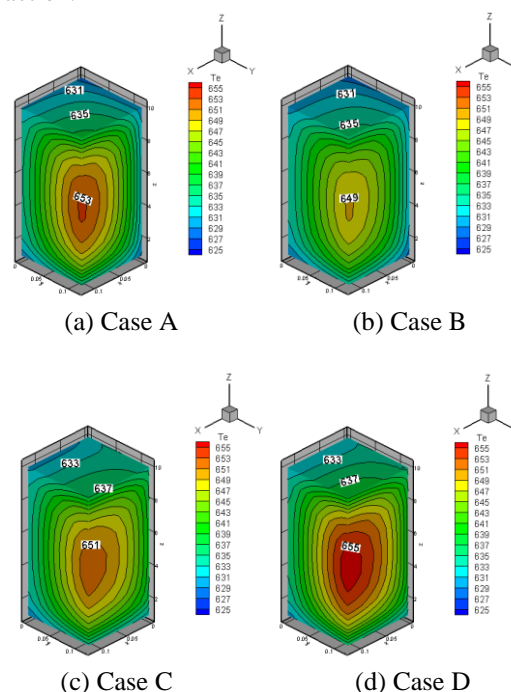


Fig. 3 Cell temperature distribution with or without reforming and water-shift reactions when the fuel inlet mole flow rate is 0.09 mol/s, (a) without reforming and water-shift reaction, (b) with reforming and without water-shift reaction, (c) with reforming and water-shift reaction, (d) without reforming and with water-shift reaction.

Figure 4 depicts the average current density, average cell temperature, current density deviation, and cell temperature deviation of the SOFC stack. In the Fig. 4(a), the case C has the highest average current density because this case includes both the reforming and water-shift reaction, which can produce more hydrogen through these reactions. As the same reason, case A has the lowest average current density because it has not the two reactions. In the case B and D, the average current density is dependable to the reaction rate of the reforming and water-shift reaction. In Fig. 4(b), case D has the

highest temperature because the reforming reaction is endothermic and the water-shift reaction is exothermic. As the same reason, case B only includes the reforming reaction, so it has the lowest average cell temperature. The case C includes both the reforming and water-shift reaction and its average cell temperature is similar to that of case A, which has not the two reactions. The average cell temperature of case C is higher than that of case A when the reforming reaction rate is lower than that of water-shift reaction. Moreover, the reforming and water-shift reaction will promote the power of the SOFC, and slightly change the average cell temperature through comparing the Fig. 4(a) and 4(b). Thus, these two reactions are advanced for a SOFC stack. In Fig. 4(c), the case B and C including the reforming reaction have lower current density deviation, and these two cases have about 50 A/m² drop related to the case A and D. The reforming reaction can effectively drop the current density deviation, and this result is good for a fuel cell. In Fig. 4(d), the trend is similar to that in Fig. 4(c), because the cell temperature depends on the electrochemistry reaction heat, which is related to the current density. In this figure, the case B and C have lower temperature deviation, and there are about 5 °C gap related to the case A and D. In a fuel cell, the temperature deviation will induce the non-uniform thermal stress and decreases the fuel cell life when the derivation is large. Concluding the result of Fig. 4(a) to 4(d) indicates that the reforming reaction and water-shift reaction can effectively promote the total power and drop the current density deviation, but slightly affect the average cell temperature and cell temperature deviation.

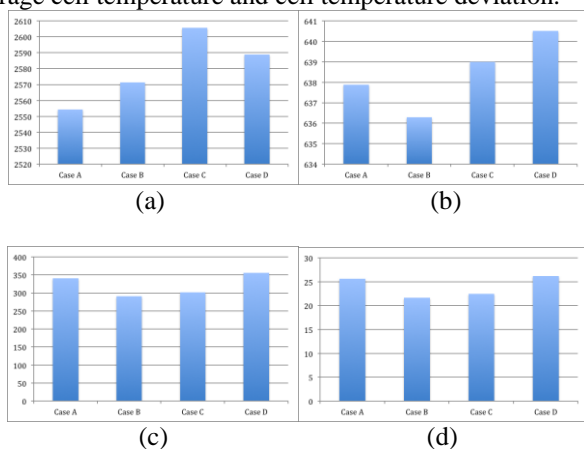


Fig. 4 Histogram analysis of the performance of a SOFC stack
(a) Average current density (b) Average cell temperature (c)
Current density deviation (d) Cell temperature deviation

iv. Conclusions

This study investigates the effect of reforming and water-shift reaction on the thermal and electrical performance of a SOFC with 10 stacks. Through the accuracy comparison, this study utilizes a reliable software to calculate the mass conservation equations, energy conservation equations, and electrochemistry equations, simultaneously, as well as gets the values of important variables such as the cell temperature and current density. The results show that the reforming reaction

and water-shift reaction can effectively promote the total power and drop the current density deviation, but slightly affect the average cell temperature and cell temperature deviation. Thus, these two reactions are advanced for a SOFC stack.

Acknowledgment

The authors would like to thank the National Science Council of the Republic of China, Taiwan, for the financial support of this research under Contract No. NSC 102-2221-E-234-002.

References

- [1] J.R. Ferguson, J.M. Fiard, R. Herbin, Three-dimensional numerical simulation for various geometries of solid oxide fuel cells, *J. Power Sources*, vol. 58, pp. 109-122, 1996.
- [2] H. Yakabe, M. Hishinuma, M. Uratani, Y. Matsuzaki, I. Yasuda, Evaluation and modeling of performance of anode-supported solid oxide fuel cell, *J. Power Sources*, vol. 86, pp. 423-431, 2000.
- [3] V.M. Janardhanan, V. Heuveline, O. Deutschmann, Performance analysis of a SOFC under direct internal reforming conditions, *Journal of Power Sources*, 172 (2007) 296-307.
- [4] E. Achenbach, Three-dimensional and time-dependent simulation of a planar solid oxide fuel cell stack, *J. Power Sources*, vol. 49, pp. 333-348, 1994.
- [5] K.P. Recknagle, R.E. Williford, L.A. Chick, D.R. Rector, M.A. Khaleel, Three-dimensional thermo-fluid electrochemical modeling of planar SOFC stacks, *J. Power Sources*, vol. 113, pp. 109-114, 2003.
- [6] S.B. Beale, Y. Lin, S.V. Zhubrin, W. Dong, Computer methods for performance prediction in fuel cells, *J. Power Sources*, 118 (2003) 79-85.
- [7] W.J. Sembler, S. Kumar, Modification results from computational-fluid-dynamics simulations of single cell solid oxide fuel cells to estimate multicell stack performance, *Journal of Fuel Cell Science and Technology*, 8 (2011) 021008.
- [8] M. Peksen, A coupled 3D thermofluid-thermomechanical analysis of a planar type production scale SOFC stack, *International Journal of Hydrogen Energy*, 36 (2011) 11914-11928.
- [9] G. Brus, J. S. Szmyd, Numerical modelling of radiative heat transfer in an internal indirect reforming-type SOFC, *Journal of Power Sources* 181 (2008) 8-16
- [10] M. Peksen, R. Peters, L. Blum, D. Stolten, Numerical modelling and experimental validation of a planar type pre-reformer in SOFC technology, *international journal of hydrogen energy* 34 (2009) 6425-6436.
- [11] K.P. Recknagle, E.M. Ryan, B.J. Koepfel, L.A. Mahoney, M.A. Khaleel, Modeling of electrochemistry and steam-methane reforming performance for simulating pressurized solid oxide fuel cell stacks, *Journal of Power Sources* 195 (2010) 6637-6644.
- [12] J. Xu, G.F. Froment, Methane steam reforming, methanation and water-gas shift: I. Intrinsic kinetics, *AIChE Journal* 35 (1989) 88-96.
- [13] Y. Choi, H.G. Stenger, Water gas shift reaction kinetics and reactor modeling for fuel cell grade hydrogen, *Journal of Power Sources* 124 (2003) 432-439.
- [14] J. Zou, J. Huang, W.S. Winston Ho, CO₂-Selective Water Gas Shift Membrane Reactor for Fuel Cell Hydrogen Processing, *Ind. Eng. Chem. Res.* 46 (2007) 2272-2279.

- [15] Syu-Fang Liu, Mu-Sheng Chiang, Shih-Bin Wang, Ping Yuan, Electrical and thermal performance of a solid oxide fuel cell unit with non-uniform inlet flow and high fuel utilization, *Fuel Cell Science and Technology*, 8 (2011) 031002-1-7.
- [16] P. Yuan, Effect of inlet flow maldistribution in the stacking direction on the performance of a solid oxide fuel cell stack, *Journal of Power Sources* 185 (2008) 381-391.
- [17] Ping Yuan and Syu-Fang Liu, Numerical Analysis of Temperature and Current Density Distribution of a Planar Solid Oxide Fuel Cell Unit with Non-uniform Inlet Flow, *Numerical Heat Transfer, Part A* 51 (10) (2007) 941-957.

About Author (s):



Ping Yuan is a professor of mechanical engineering at Lee Ming Institute of Technology. He received his Ph.D. (1999) in mechanical engineering from Tatung University in Taiwan. His research areas includes heat and mass transfer, fuel cell analysis, and bio-heat transfer.